

## FIRST EXPERIMENTAL RESULTS ON FORCED-CONVECTION HEAT TRANSFER INSIDE A WAVY CHANNEL

Damiano Fustinoni, Pasqualino Gramazio, Alfonso Niro

Dipartimento di Energia, Politecnico di Milano, Campus Bovisa, via Lambruschini, 4 – I-20156 Milano, Italy

### ABSTRACT

In this paper we present the results of an experimental investigation on average heat transfer characteristics and pressure drops of a forced air-flow through a rectangular channel with the lower and upper walls wavy configured. The test section is 880-mm long, 120-mm wide and 12-mm height, whereas waviness have in streamwise direction a triangular profile of 68-mm pitch and  $161^\circ$  apex angle; this geometry reproduces in a larger-scale a typical passage between two wavy-fins in a compact heat exchanger. The channel is operated with the wavy walls at uniform temperature whereas the side ones are adiabatic.

Results here presented are for a wavy-wall temperature of  $40^\circ\text{C}$ , air inlet-temperature of near  $20^\circ\text{C}$ , and Reynolds numbers ranging from about 700 to 7500. Comparisons with the results specifically obtained in a flat rectangular channel, with the same dimensions and operating conditions, show that for the investigated wavy channel the laminar-to-turbulent transition starts at lower values of the Reynolds number, i.e., 1350, and heat transfer is enhanced from 40% to 80% but with a pressure penalization larger than 60%.

### INTRODUCTION

Heat transfer in air forced convection over enhanced surfaces is a very interesting matter since it is encountered in devices largely used such as compact heat exchangers, as well as in critic applications like turbine blade cooling. In designing compact heat exchangers, high values of heat transfer area per unit volume are looked for; however, increasing this parameter over a given value, thermal performances start worsening. Indeed, the higher the surface-to-volume ratio, the narrower the passages, and hence the air velocity has to be lowered to maintain acceptable pressure drops; in turn, narrow passages and low air velocities induce a laminar or weakly turbulent flow that is characterized by a quite poor convective coefficient which eventually defeats completely the area increase benefits. In order to overcome this limit, designer enhances heat transfer using specially configured extended-surfaces, such as offset or louvered or wavy fins, which are an efficient and cost-effective solution.

As the shape of these structured extended-surfaces depends on the enhancement mechanisms employed, there is a large variety of geometries and consequently a large number of studies in the literature (Webb [1] reports near 40 papers). More precisely, several correlations deal with the offset and louvered fins (Joshi and Webb [2], Wieting [3], Davenport [4]), whereas the wavy-fin geometry is suffering from a some lack of data as well as of relevant correlations yet. For this reason, the authors are currently involved in an investigation on heat transfer characteristics of forced convection inside wavy channels.

This paper reports on the results of average convective coefficients and pressure drops of air-flows in a wavy channel with a geometry reproducing in a larger-scale a typical passage inside a wavy-fin compact heat exchanger for Reynolds numbers ranging from about 700 to 7500. These results are also compared with data specifically obtained in a flat channel with the same dimensions and at the same operating conditions as the wavy channel.

### EXPERIMENTAL SETUP

As schematically shown in Figure 1, the experimental setup consists of two independent circuits, namely, the air-circuit containing the test section, and the heating-water circuit used to control the temperature of the channel walls.

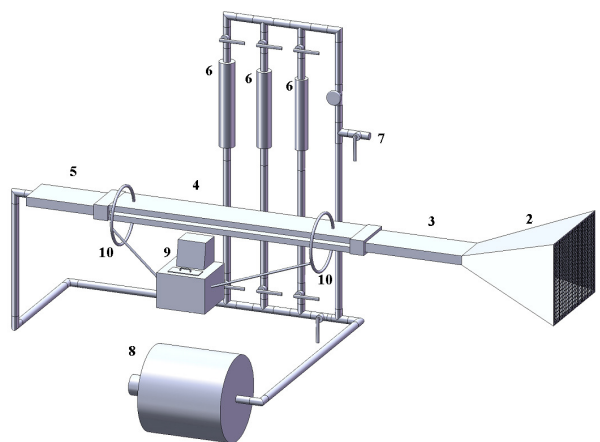


Figure 1. Schematics of the experimental setup: 1. fine mesh screen cover; 2. convergent air inlet; 3. entry-section; 4. test-section; 5. exit-section; 6. rotameters; 7. by-pass; 8. blower; 9. heat bath; 10. water circuit piping.

Through a convergent, room air flows into the circuit; a fine mesh screen covers the convergent inlet whereas at its outlet there is a flow straightener consisting in a matrix of staggered 4-mm-diameter, 40-mm long thin polystyrene tubes. Inside the convergent a thermo-resistance, i.e., a resistance thermometer, is mounted to measure the air temperature. From the straightener air flows into an entry-section that is a rectangular duct with the same cross dimensions as the tested channel; entry-section is 0.4-m long, i.e., near 20 times the channel hydraulic diameter, and its

walls are made with 10-mm thick plexiglas plates and are not heated. At the end of this section, air enters the test-section that is a 120-mm wide, 12-mm height, 880-mm long duct; its lower and upper walls are two aluminium plates of 10-mm minimum thickness with a wavy configured face.

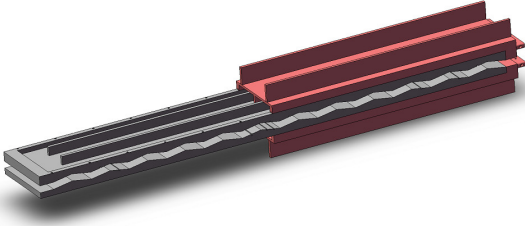


Figure 2. Test section with the duct on the wall backside.

As shown in Figure 2, the backside of each plate is covered by a cap strongly tightened to the plate, so that they form a jacket where the heating water flows. Inside and outside the water jacket there are ribs which prevent the plate buckling. To check if temperature is uniform over the heated walls, six thermocouples are embedded in the lower wall and four in the upper one; each thermocouple is cemented into a 1.8-mm-wide, 0.5-mm-depth groove cut in the face with waviness; thermocouple locations are displayed in Figure 3 whereas Table 1 lists the exact position of their junctions. Eventually, the test-section sides are closed by 4-mm-thick glass plates to allow optical access inside the channel.

Table 1. Probe positions on wavy channel wall.

<i>Upper wall</i>			<i>Lower wall</i>		
	<i>x</i>	<i>y</i>		<i>x</i>	<i>y</i>
	[mm]	[mm]		[mm]	[mm]
1	110	60	1	85	60
2	410	30	2	150	60
3	450	30	3	420	90
4	790	60	4	430	45
			5	460	90
			6	700	60

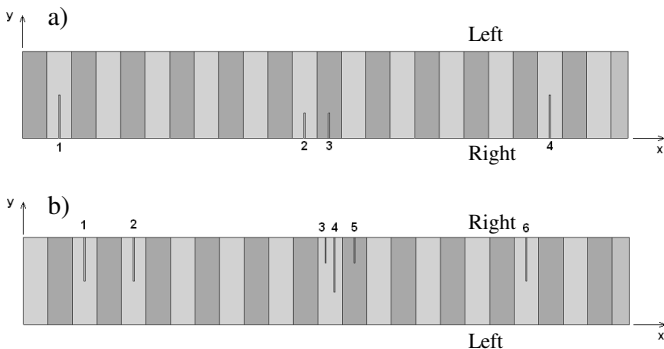


Figure 3. Thermocouples locations on upper (a) and lower (b) test channel walls

At the test-section outlet, there is a short exit-section equipped first with two turbolizer rows and then with a convergent that conveys air through a 20-mm-wide, 6-mm-high channel partially filled by a fine-meshed plastic net; after the screen a thermo-resistance and a thermocouple are

positioned on the axis of this channel in order to measure the air bulk-temperature. Finally, inside the couplings between the entry-section and the test-section, and between this one and the exit-section there are two pressure taps, each consisting in a 1.5-mm-diameter hole (great care was devoted in eliminating any burr). Downstream the exit-section there are three rotameters, i.e., float-type flow-meters, connected in parallel with full scale of 6, 23.5 and 40 m<sup>3</sup>/h respectively, a metering valve, and a 7-stage, 30-kPa-head, 5.5-kW-power blower operating in suction mode. The exhausted air is discharged outside the laboratory. Air temperature is also measured upstream the flow-meters by means of a thermocouple plugged in the pipe.

The heating circuit is mainly composed by a heat bath which provides a high mass flow-rate of water at constant temperature, and by the channels built into the upper and lower test-section walls (water and air stream in counterflow); two thermocouples are placed inside each water channel, near the inlet and outlet ports, respectively. The heat bath is the ThermoHaake B12 with a tank of 12-dm<sup>3</sup>, a 3-kW heater and a high precision controller; water temperature inside the tank is kept constant within 0.01 K.

## MEASUREMENTS, DATA PROCESSING AND ERROR ANALYSIS

The thermocouples used are T-type with 0.5-mm-diameter wires, whereas the thermo-resistances are 4-wires, 100-ohm, Platinum type, i.e., PT100, with dimensions of 2 mm x 4 mm. Both thermocouples and thermo-resistances were all preliminary calibrated over five points within the temperature range from 22 to 60 °C, by means of the ThermoHaake heat bath. The probes were immersed all together into the bath while devoting great care in their positioning; for each calibration point, 160 readings per probe were collected; the resulting standard deviation is of 0.02 K for the thermocouples, and of 0.01 K for the thermo-resistances. All temperature measurements are performed by means of an Agilent 34970A data logger equipped with a relay multiplexer and a 6½ digit multimeter. The channels are sequentially read, by waiting a 0.5-s settling time after each channel-locking, with an integration time of 400 ms which ensures a standard deviation of 0.01 K that is less than or equal to the probe uncertainties; consequently, reading cycles are performed every 20 s. Pressure drops are measured by connecting the two pressure taps, placed at the inlet and outlet of the test channel, to a differential micromanometer with a full scale of 250 Pa and a 0.125-Pa sensitivity. Air volume-flow-rate is measured by means of the aforementioned rotameters which have a 2% nominal accuracy; however, by means of a calibration performed by measuring pressure drops of laminar air-flows through a smooth circular tube, we found that their accuracy is better of 1%. Finally, in order to guarantee repeatability to measurements, we adopted a precise test procedures described in the following. First, we power the bath heater and water starts to circulate through the entire circuit included the ducts on the test-section wall backside. After 30 m, that is the time to stabilize the channel wall temperature to a prefixed value within a 0.01-K band, we power the blower and air starts to flow through the test section. Then we need to wait for other 30 m in order to attain regime conditions with all temperature time-fluctuations within 0.02-K band; in this conditions, channel wall-temperature is uniform within 0.1 K over the entire heated length. Eventually, we start to collect 20 reading-cycles which take 400 s; during this time, measurements of the

air-volume-flow-rate and of reading-cycles was chosen first by collecting data for  $N=200$  for some of the most representative regime conditions, and then by calculating their average standard deviation as a function of  $N$ ; as a result, we found that at  $N=20$  the average standard deviation becomes less than 0.01 K, and thus we assumed that 20 is the minimum reading-cycle number to be collected.

The average Nusselt over the test section and the apparent Darcy friction factor are calculated as follows:

$$Nu = \frac{D_h}{k} \frac{\rho V c_p}{A_s} \ln \frac{\theta_i}{\theta_o} \quad (1)$$

$$f = \frac{2 \Delta p A^2 D_h}{\rho V^2 L \ell_{taps}} \quad (2)$$

where  $V$  the air volume-flow-rate,  $\rho$  the density calculated at the temperature where  $V$  is measured,  $c_p$  the specific heat at constant pressure,  $k$  the thermal conductivity,  $A_s$  the total heated area,  $\theta_i$  and  $\theta_o$  the wall-to-air-bulk-temperature difference at the test section inlet and outlet respectively,  $D_h$  the hydraulic diameter,  $\Delta p$  the measured pressure drop, and  $\ell_{taps}$  the distance between the pressure taps.

By combining the above reported uncertainties affecting the various amounts in Equations 1 and 2, eventually we evaluate the error on convective coefficient is less than 3%, whereas the error on the apparent Darcy friction factor is less than 5% for the wavy while becoming slightly larger, i.e., 6.6%, for the rectangular channel with flat walls.

## RESULTS

Experimental results here presented refer to a wavy channel whose geometry is schematically shown in Figure 4 whereas its main geometrical parameters are listed in Table 2. All data are for fixed and uniform wall-channel-temperature at the nominal value of 40 °C, and for air-flows entering into the test-section at room temperature of near 22 °C (elaborations, indeed, account for their actual values).

Table 2. Wavy channel geometrical parameters.

$h$	[mm]	12.00
$a$	[mm]	5.69
$l$	[mm]	68.00
$\alpha$	[°]	161.00
Channel width	[mm]	120.00
Hydraulic diameter	[mm]	21.82
Height to width ratio	[-]	0.10
Waviness number	[-]	12
$A_s$	[m <sup>2</sup> ]	0.2043

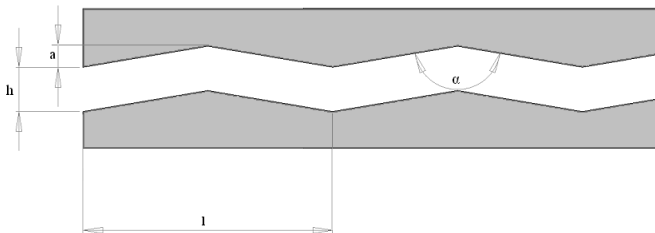


Figure 4. Wavy channel geometry.

In Figure 5 the average Nusselt number over the test section, evaluated according to Equation 1, is plotted versus

the Reynolds number. Values obtained for the flat channel, operated at the same conditions, are plotted for comparison. As it can be seen, for the wavy channel the average Nusselt number is practically a constant as for the flat channel, with essentially the same value of 7.9. However, at  $Re=1350$  the average Nusselt number for the wavy channel starts to increase exhibiting a power-law dependence on the Reynolds number with an exponent of about 0.8 (somewhat less for  $Re>3230$ ). For the flat channel, instead, the average Nusselt number remains a constant at least for Reynolds number up to 2100. For comparison, the figure also reports as solid lines the values calculated for a flat rectangular-channel by means of the correlation of Shah and London with Wibuldas correction for  $Re<2300$ , and the one of Gnielinski for  $Re\geq 2300$  [10]; all predictions take into account thermal effects of the entry-region. As seen, present data agree very well with predictions.

From these trends, we infer that the waviness promotes turbulence and advances the laminar-to-turbulent transition. At  $Re=7530$ , i.e., at the upper limit of the investigated range of flow-rates, the wavy channel exhibits an average Nusselt number 25% larger than for the flat channel at the same Reynolds number, although heat transfer enhancement seems to decrease with  $Re$  (this effect should be consistent with the fact that waviness effectiveness in promoting turbulence also decreases as  $Re$  increases since the larger  $Re$  the smaller the structures).

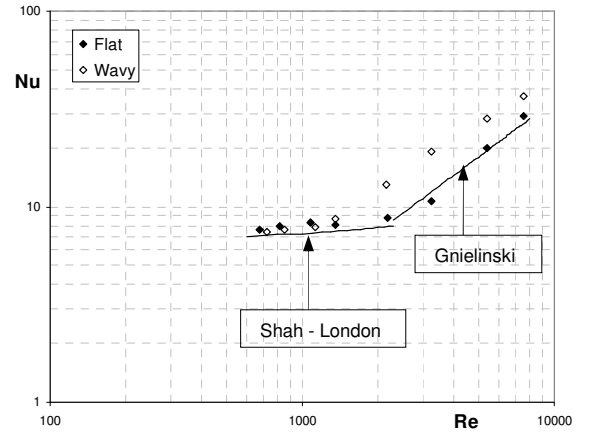


Figure 5. Average Nusselt number versus Reynolds number.

Figure 6 shows the experimental values of the apparent Darcy friction factor  $f$  plotted versus the Reynolds number both for the wavy channel and for the flat channel. For comparison, the figure also reports as solid lines the values calculated for a laminar-flow by means of the correlation proposed by Shah and London [10]. For the wavy channel,  $f$  displays a trend similar to that for the flat channel in laminar-flow but with 57% larger values. As it can be seen, also  $f$  points out a early laminar-to-turbulent transition, although its onset seems to occur at slightly larger value of  $Re$ . For fully turbulent-flow,  $f$  seems to take again the same dependence on  $Re$  as that for the flat channel but with 82% larger values. Finally, the experimental data for the flat channel agree very well with literature predictions.

As a concluding remark, from an engineering point of view it is interesting to compare the overall performance of the wavy channel with respect to the flat channel by taking into account both heat transfer enhancement and pressure-drop penalization. Currently there are several criteria to carry out this comparison, but here we consider the two most popular. The first one, which we refer to as Criterion A, performs comparisons by keeping constant the mass flow-rate, i.e., at

the same Reynolds number. According to the second one, Criterion B, comparisons are done by fixing the power required by the pump/blower. Figure 7 shows a graph where the values calculated by the three criteria are plotted versus the Reynolds number. As shown, indications from the two criteria are characterized by similar trends but different values.

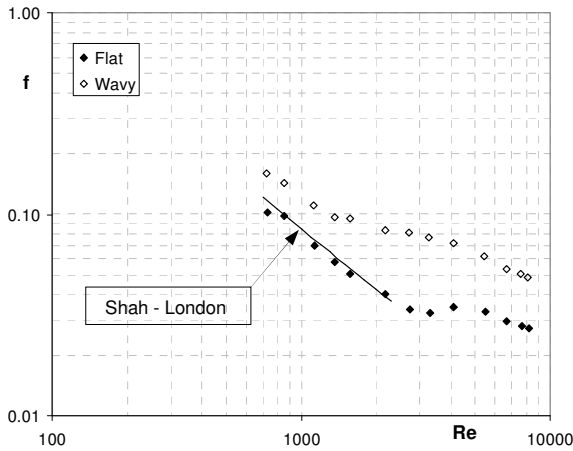


Figure 6. Darcy friction factor versus Reynolds number.

Anyway, both criteria agree in pointing out the wavy-channel overall performances are unfavourable for  $Re < 1350$  while becoming interesting within the range from 2000 to 5000. For larger values of  $Re$ , overall performances comes back to be poor.

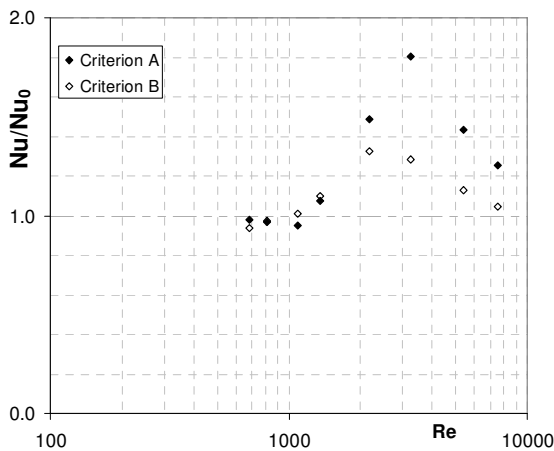


Figure 7. Ratio between  $Nu$  for wavy channel and a reference value evaluated for a flat channel at fixed mass flow rate (Criterion A) or at fixed pumping power (Criterion B), versus Reynolds number.

## CONCLUSIONS

This paper reports about an experimental investigation on heat transfer characteristics of an airflow inside a wavy channel at Reynolds numbers between 700 and 7530. The enhancement effect is essentially due to the periodic streamline deflection induced by the wall waviness. The heat transfer measurements over the entire channel show the flow is laminar up to  $Re=1350$ ; within this regime, the average Nusselt number is independent of the Reynolds number, as for the smooth channel case, and with the same value.

In spite to these enhanced heat transfer characteristics, however, the apparent Darcy friction factor worsens of nearly 60%. At  $Re=1350$ , flow regime becomes early transitional with respect to the flat channel. This event is well pointed out by a slope change in the average Nusselt number trend which from a constant becomes a power-law increasing function of the Reynolds number with an exponent of 0.8. The transitional flow regime is characterized by an increase of the heat transfer coefficient as well as of the apparent friction factor with respect to the flat channel. Finally, for  $Re \geq 3230$  flow becomes fully turbulent, the growth of the average Nusselt number with  $Re$  attenuates the exponent of the letter lowers to 0.8, and the apparent friction factor display a trend similar to the flat channel. Consequently at  $Re=7530$ , i.e., the upper limit of the  $Re$  investigated range, the present wavy channel is characterized by an enhancement increasing of 25% but with a 80% larger friction factor.

## ACKNOWLEDGMENT

This work is supported by MURST (the Italian Ministry for the University and the Scientific-Technical Research) via PRIN 2007 grants.

## NOMENCLATURE

Symbol	Quantity	SI Unit
$A_S$	Total heated area	$m^2$
$D_h$	Hydraulic diameter	$m$
$V$	Volume flow rate	$m^3/s$
$c_p$	Specific heat	$J\ kg^{-1}\ K^{-1}$
$f$	Darcy friction factor	
$k$	Thermal conductivity	$W\ K^{-1}\ m^{-1}$
$\ell_{taps}$	Distance between pressure taps	$m$
$\Delta p$	Pressure drop	$Pa$
Greek symbols		
$\theta$	Wall-to-air-bulk-temperature difference	$^{\circ}C$
$\rho$	Density	$kg/m^3$
Subscripts		
$i$	inlet	
$o$	outlet	

## REFERENCES

- [1] R. L. Webb, Principles of Enhanced Heat Transfer, John Wiley & Sons, cap. 9, pp. 228-284, 1994.
- [2] M. Fiebig, "Vortices: tools to influence heat transfer. Recent developments", Proc. 2nd European Thermal Sciences and 14th UIT National Heat Transfer Conference, vol. 1 pp. 41-56, Rome, June 1996.
- [3] W. M. Kays, Compact Heat Exchangers, AGARD Lecture Ser. No. 57 on Heat Exchangers, ed. Ginoux, AGARD-LS-57-72, Jan. 1972.
- [4] H. M. Joshi, R.L. Webb, Prediction of heat transfer and friction in the offset strip fin array, Int. Journal of Heat and Mass Transfer, Vol. 30, No. 1, pp. 69-84, 1987.
- [5] A. R. Wieting, Empirical correlations for heat transfer and flow friction characteristics of rectangular offset fin

- heat exchangers, J. Heat Transfer, Vol. 97, pp. 488-490, 1975.
- [6] C. J. Davenport, Correlations for heat transfer and flow friction characteristics of louvered fin, Heat transfer-Seattle 1983, AIChE Symp. Ser., No. 225, Vol. 79, pp. 19-27, 1984.
  - [7] L. J. Goldstein, E. M. Sparrow, Heat/mass transfer characteristics for flow in a corrugated wall channel, J. Heat Transfer, Vol. 99, pp. 187-195, 1977.
  - [8] M.M. Ali, S. Ramadhyani, Experiments on convective heat transfer in corrugated channels, Experimental Heat Transfer, Vol. 5, pp. 175-193, 1992.
  - [9] S. W. Chang, A. W. Lees, and T. C. Chou, Heat transfer and pressure drop in furrowed channels with transverse and skewed sinusoidal wavy walls, Int.J.Heat Mass Transfer 19-20 (52), pp. 4592-4603, 2009.
  - [10] S. Kakaç, R. K. Shah, W. Aung, Handbook of single-phase convective heat transfer, Wiley-Interscience, 1987.